# INCORPORATING COLOR INFORMATION FOR RELIABLE PALMPRINT AUTHENTICATION

*Aythami Morales[1, 2], Ajay Kumar[2], Miguel A. Ferrer[1]*

[1] Instituto para el Desarrollo Tecnológico y la Innovación en Comunicaciones (IDeTIC). Universidad de Las Palmas de Gran Canaria, Las Palmas de Gran Canaria, Spain

[2]Department of Computing, The Hong Kong Polytechnic University, Hung Hom, Kowloon, Hong Kong

**ABSTRACT**

This paper investigates new approaches for improving the conventional palmprint authentication performance by integrating color information. We firstly propose a new approach for image level combination of multiple color components to generate more reliable palmprint representation than the conventional gray level representation. This investigation is motivated to develop more robust palmprint representation that can be employed to achieve better performance for the conventional palmprint identification, with the same computational complexity. Secondly, this paper presents a rigorous analysis of different color representations for the palmprint images to ascertain the performance improvement using different feature representations (OLOF and SIFT) and different databases (scanner and webcam). The rigorous experimental results from this study suggest that the influence of color information can differently alter the performance gain, which varies with the nature of employed feature representation.

***Index Terms—*** Biometrics, color palmprint, image fusion.

## 1. INTRODUCTION

Automated palmprint identification using palmprint images has been extensively studied in the literature. However almost all of the palmprint identification approaches exploit the gray-level images and there has been very little or negligible efforts to improve the palmprint identification using color information.

The random texture patterns exploited for the discriminative palmprint identification are often associated with color information. Historically, the lower cost of grayscale imaging and computing hardware have justified the popular choice of grayscale images for the algorithm development and deployment. The availability of low-cost color cameras and computing hardware is motivating more researchers and developers to exploit color information in achieving improved performance.

There have been prior efforts to explore the use of color information in improving the palmprint authentication. Reference [3] proposes the palmprint feature extraction method based on the color of the palm skin. This approach uses the color as feature to ascertain the authentication performance and illustrates promising results on the proprietary database. In reference [4], the DCT based feature extraction approach is employed from the different color component images. The score level fusion of palmprint images in different color components has shown to improve the respective grayscale results on a proprietary database.

The use of color information from palmprint images for the more popular and effective gray-level feature representation is yet to be explored. Such investigation should also ascertain the variation in the performance improvement, if any, from various feature representations and from the different imaging conditions (or databases).

## 2. OUR APPROACH

In this paper we investigate the usage of color information to improve the performance for the two highly promising palmprint features [1]-[2]. In particular, we propose two approaches to integrate the color information to improve the performance from the conventional approaches:

- Gray level representation for palmprint image using a unique combination of *RGB* components from color representation.
- Comparative study of different color representations and their score level combination for the palmprint authentication.

Our study presented in this paper suggests that the simultaneous use of color information can offer improved performance than the conventional approaches. We present experimental results from the two public databases with more than 5000 palmprint images from 1394 users acquired with two different sensors in controlled and uncontrolled conditions. The nature of employed database helps us to investigate the influence of sensor, acquisition conditions and nature of extracted features for the usability of color information.

## 3. FEATURE EXTRACTION APPROACHES

In this paper we used two of the most promising palmprint approaches based on global and local information of the palmprint. The Scale Invariant Feature Transform [1], [8] (SIFT) as approach based on local information and Orthogonal Line Ordinal Features [2] (OLOF) as global appearance or texture approach.

### 3.1. Modified Scale Invariant Features Transform (MSIFT)

This approach is based on application of SIFT algorithm to 2D Gabor filter enhanced palmprint images [5]. The features extracted are invariant to image scaling, rotation, and partially invariant to change in illumination and projective distortion.

The SIFT algorithm is based on the study of information around several keypoints in palmprint images. The keypoints selection and characterization is done following three steps [6]:

**1**. Scale-space extrema detection: The I(x, y) Gabor enhanced input image is transformed to:

$$L(x,y,\sigma) = N(x,y,\sigma) * I(x,y)$$

where $*$ corresponds to convolution operator and $N(x,y,\sigma)$ is a Gaussian function with bandwidth σ.

**2.** Keypoint localization: The keypoints $c_i = \{x_i, y_i\}$ are obtained evaluating the maxima and minima of the difference-of-Gaussian function:

$$D(x,y,\sigma) = L(x,y,k\sigma) - L(x,y,\sigma)$$

The number of keypoints selected depends on the palmprint image. Therefore if we consider each color components as independent image the number and location of keypoint depends on the employed color component (figure 1).

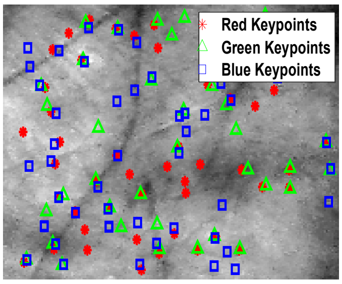


**Figure 1: Localization of SIFT keypoints for red, green and blue components of the same palmprint image.**

**3.** Keypoint descriptor: each keypoint $c_i$ is defined by a descriptor vector $d_i$ containing the orientations and gradients magnitudes around the keypoints coordinates.

The verifier evaluates the number of matches between test and training images based on Euclidean distance of the keypoint descriptors vectors.

### 3.2. Orthogonal Line Ordinal Features (OLOF)

The Orthogonal Line Ordinal Features method was originally introduced in [2]. This method is based on 2D Gaussian filter to obtain the weighted average intensity of a line-like region. Its expression is as follows:

$$f(x,y,\theta) = exp\left[-\left(\frac{xcos\theta + ysin\theta}{\delta_x}\right)^2 - \left(\frac{-xsin\theta + ycos\theta}{\delta_y}\right)^2\right]$$

where θ denotes the orientation of 2D Gaussian filter, $\delta_x$ denotes the filter's horizontal scale and $\delta_y$ denotes the filter's vertical scale parameter. We empirically selected the parameters as $\delta_x = 5$ and $\delta_y = 1$.In order to obtain the orthogonal filter, two Gaussian filters are used as follows:

$$OF(\theta) = f(x,y,\theta) - f\left(x,y,\theta + \frac{\pi}{2}\right)$$

Each of the palmprint image is filtered using three ordinal filters, *OF(0), OF(π/6),* and *OF(π/3)* to obtain three binary masks based on a zero binarization threshold. In order to ensure the robustness against brightness, the discrete filters *OF(θ)*, are turned to have zero average. Once filtered the palm image are resized to 50 × 50 pixels. The figure 2 shows the three overlapped masks for red, green and blue components of a RGB palmprint image.

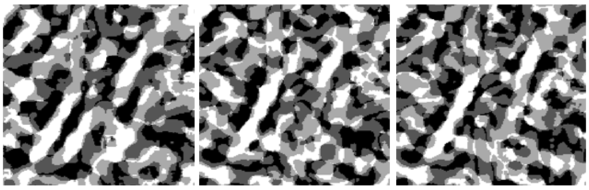

**Figure 2: From left to right: red, green and blue OLOF masks of the same palmprint image.**

The matching distance between the palmprint image feature matrix *Q* and the palmprint image feature matrix *P* (say reference template) is computed by the normalized Hamming distance which can be described as follows:

$$D = 1 - \frac{\sum_{i=1}^{2n+1}\sum_{j=1}^{2n+1} P(i,j)\otimes Q(i,j)}{(2n+1)^2}$$

where the boolean operator $\otimes$ is the conventional XOR operator. The numeric value of *D* ranges lies between 0-1 and the best matching is achieved when the value of *D* is 1. In order to accommodate high intra-class variations from the imaging and imperfections in the preprocessing, vertical and the horizontally translation ordinal feature map is used to ascertain the best possible matching score. The ranges of the vertical, horizontal traslations and rotations are empirically determined and were fixed as from -6 to 6. The maximum *D* value obtained from such multiple translated matching is assigned as the best or final matching score.

## 4. GREY LEVEL REPRESENTATION

Conversion of a color image to grayscale is not unique; different weighting of the color components conventionally represents the effect of imaging monochrome film with different-colored photographic filters in the camera. A common strategy is to match the luminance of the grayscale image to the luminance of the color image. To convert *RGB* color components to a grayscale representation of its luminance, following equation is commonly employed:

$$I_{gray}(x,y) = 0.30 I_R(x,y) + 0.59 I_G(x,y) + 0.11 I_B(x,y)$$

with $I_R(x,y), I_G(x,y), I_B(x,y)$, $0 \leq I(x,y) \leq 1$ being the red, green and blue components of the RGB image. A general form of this equation can be rewritten as follows:

$$I_{gray}(x,y) = w_1 I_R(x,y) + (1 - w_2 - w_1) I_G(x,y) + w_2 I_B(x,y)$$

where $w_1$ and $w_2$ the weighting factors and $I_R(x,y), I_G(x,y), I_B(x,y)$, $0 \leq I(x,y) \leq 1$, $1 \leq x \leq 800$, $1 \leq y \leq 600$ in our experiments. Different weights empathize different color components. In this paper, we investigate how a unique selection of color component combination could outperform the conventional grayscale approach.

## 5. COLOR REPRESENTATIONS

The second set of investigation in this paper is based on the study of usability of *RGB*, *HSV* and *YCbCr* color spaces. A color space is an abstract mathematical model describing how the color information can be represented by numbers.

*RGB* color space is defined by the three chromaticities of the red, green, and blue additive primaries, and can produce any chromaticity that is the triangle defined by those primary colors.

*YCbCr* is not an absolute color space, it is an alternative approach of encoding *RGB* information. A value expressed as *YCbCr* is only predictable if standard *RGB* components are used. *Y* is the luminance, meaning that light intensity is non-linearly encoded using gamma correction. *Cb* and *Cr* are the blue-difference and red-difference chroma components. In this paper we used an *YcbCr* transformed space based on equations:

$$I_Y(x,y) = 0.299 I_R(x,y) + 0.587 I_G(x,y) + 0.114 I_B(x,y)$$
$$I_{Cb}(x,y) = -0168736 I_R(x,y) - 0.331264 I_G(x,y) + 0.5 I_B(x,y)$$
$$I_{Cr}(x,y) = 0.5 I_R(x,y) - 0.418688 I_G(x,y) - 0.081312 I_B(x,y)$$

*HSL* and *HSV* are the two most common cylindrical-coordinate representations of points in an *RGB* color model, which rearrange the geometry of *RGB* in an attempt to be more perceptually relevant than the cartesian representation. In this paper we used an *HSV* transformed space based on equations:

$$I_H(x,y) = \begin{cases} not\ defined, & if\ Max = Min \\ 60° \times \dfrac{I_G(x,y) - I_B(x,y)}{Max - Min}, & if\ Max = I_R(x,y) \\ & and\ , I_G(x,y) \geq I_B(x,y) \\ 60° \times \dfrac{I_G(x,y) - I_B(x,y)}{Max - Min} + 360°, & if\ Max = I_R(x,y) \\ & and\ , I_G(x,y) < I_B(x,y) \\ 60° \times \dfrac{I_B(x,y) - I_R(x,y)}{Max - Min} + 120°, & if\ Max = I_G(x,y) \\ 60° \times \dfrac{I_R(x,y) - I_G(x,y)}{Max - Min} + 240°, & if\ Max = I_B(x,y) \end{cases}$$

$$I_S(x,y) = \begin{cases} 0\ if\ Max = 0 \\ 1 - \dfrac{Min}{Max}\ for\ the\ rest \end{cases}$$

$$I_V(x,y) = Max$$

with $Max$ and $Min$ being the max and min of $RGB$ color components $[I_R, I_G, I_B]$.

## 6. EXPERIMENTS

We employed two different palmprint databases, which used different imaging sensors in the controlled and uncontrolled environment, to ascertain the integration of color information for the performance improvement.

The GPDS-CL2 database [5] is a real application contactless database acquired with the webcam sensor. This database consists of 110 subjects imaging with average number of images per subject as 14. The images show several pose, illumination and background variations. GPDS-CL2 database verification methodology is based on the multisession acquisition methodology. We used the first session composed by 4 images as training set and the remaining session for test. As a result, we have 1100 (110 × 10) scores for genuine and 119900 (110 × 10 × 109) scores for the impostors.

The Bogazici database [7] is another public hand database acquired with a scanner sensor. This database consists of 3 images from left and right hand from 642 users acquired in controlled illumination conditions. In our experiments we employed two images for training and rest one for the test. As a result, we have 3852 (642 × 3× 2) scores from the genuine and 2469132 (642 × 3 × 2 × 641) scores from the impostors.

## 7. RESULTS AND DISCUSSION

We now present the experimental results from the two investigated approaches for the combination of different color components.

### 7.1. New Grey Level Representation

The red, green and blue components are combined as detailed in section 3 using weighted sum and we ascertain the weights to maximize the performance. Table I and II show the results for the GPDS-CL 2 database.

**Table I. MSIFT EERs (%) for different grayscale representations using GPDS-CL2 database**

| $w_2$ \ $w_1$ | 0.1 | 0.2 | 0.3 | 0.4 | 0.5 | 0.6 | 0.7 | 0.8 |
|---|---|---|---|---|---|---|---|---|
| **0.1** | 3.10 | 3.06 | 1.95 | 1.95 | 1.63 | 1.63 | 1.77 | 1.87 |
| **0.2** | 1.84 | 1.92 | 1.84 | 1.58 | 1.50 | 1.88 | 1.70 | |
| **0.3** | 1.78 | 1.86 | 1.92 | 1.65 | 1.66 | 1.75 | | |

**Table II. OLOF EERs (%) for different grayscale representations using GPDS-CL2 database**

| $w_2$ \ $w_1$ | 0.1 | 0.2 | 0.3 | 0.4 | 0.5 | 0.6 | 0.7 | 0.8 |
|---|---|---|---|---|---|---|---|---|
| **0.1** | 2.78 | 2.89 | 2.11 | 2.16 | 2.23 | 2.29 | 2.37 | 2.46 |
| **0.2** | 2.13 | 2.14 | 2.20 | 2.26 | 2.36 | 2.47 | 2.58 | |
| **0.3** | 2.18 | 2.26 | 2.34 | 2.45 | 2.57 | 2.70 | | |

The conventional grayscale conversion approach use as weighting factors $w_1 = 0.3$, $w_2 = 0.1$. Selection of the unique color component combination (image fusion) improves the EERs by 23% and 0% for MSIFT and OLOF respectively.

Table III and IV show the results for Bogazici database using MSIFT and OLOF approaches.

**Table III. MSIFT EERs (%) for different grayscale representations using Bogazici database**

| $w_2$ \ $w_1$ | 0.1 | 0.2 | 0.3 | 0.4 | 0.5 | 0.6 | 0.7 | 0.8 |
|---|---|---|---|---|---|---|---|---|
| **0.1** | 0.72 | 0.83 | 0.87 | 0.98 | 1.13 | 1.17 | 1.29 | 1.32 |
| **0.2** | 0.73 | 0.77 | 0.93 | 1.08 | 1.17 | 1.14 | 1.39 | |
| **0.3** | 0.80 | 1.01 | 1.07 | 1.16 | 1.22 | 1.36 | | |

**Table IV. OLOF EERs (%) for different grayscale representations using Bogazici database**

| $w_2$ \ $w_1$ | 0.1 | 0.2 | 0.3 | 0.4 | 0.5 | 0.6 | 0.7 | 0.8 |
|---|---|---|---|---|---|---|---|---|
| **0.1** | 1.18 | 1.23 | 1.27 | 1.32 | 1.37 | 1.42 | 1.49 | 1.54 |
| **0.2** | 1.23 | 1.30 | 1.34 | 1.40 | 1.45 | 1.50 | 1.57 | |
| **0.3** | 1.32 | 1.39 | 1.43 | 1.48 | 1.53 | 1.60 | | |

In this case the improvement for Bogazici database is 17% and 7% for MSIFT and OLOF respectively.

The experimental results suggest that a unique weighted combination of color components can significantly improve the performance while MSIFT features are employed.

### 7.2. Combining Color Representations

Table V shows the results for the different color components *RGB*, *YCbCr* and *HSV* spaces. For these experiments we used each component as an independent image.

**Table V. EERs (%) of each RGB, YCbCr and HSV component**

| | GPDS-CL1 | | Bogazici | |
|---|---|---|---|---|
| | **MSIFT** | **OLOF** | **MSIFT** | **OLOF** |
| **Red** | 1.64 | 2.46 | 1.08 | 1.38 |
| **Green** | 2.48 | 2.07 | 1.15 | 1.40 |
| **Blue** | 4.92 | 2.55 | 1.09 | 1.59 |
| **Y** | 1.92 | 2.06 | 0.95 | 1.40 |
| **Cb** | 29.2 | 7.66 | 0.65 | 1.26 |
| **Cr** | 13.8 | 2.55 | 1.51 | 1.18 |
| **Hue** | 35.1 | 2.09 | 2.02 | 1.29 |
| **Saturation** | 6.19 | 2.61 | 0.96 | 1.30 |
| **Value** | 1.79 | 2.57 | 1.08 | 1.38 |

Table VI shows the results from the score level combination of different color components from each color space and the percentage improvement with respect to the conventional approach. The fusion of the different score is achieved using weighted sum as follows:

$$S_f = w_1 S_x + w_2 S_y + w_3 S_z$$

where $S_x$, $S_y$ and $S_z$ are three independent color components scores of *RGB, YcbCr* and *HSV* spaces and $w_1$, $w_2$ and $w_3$ are a posteriori obtained weighting factors with $0 \leq w_i \leq 1$.

## 8. CONCLUSIONS

The experimental results have illustrated that the use of color information can significantly improve the palmprint authentication performance (more than 50% improvement in EER). The experimental results have also suggested that the score level combination consistently outperforms the image level combination of color information. The *key finding of this paper* is that the commonly employed gray-scale representation for the palmprint information may not be the best and *it is possible to employ different weighted combination, with the same feature extraction and matching, and achieve better performance*. Another observation from this study is that the usage of color information is more attractive while using key point SIFT features than while using localized OLOF features.

**Table VI. EERs (%) using grayscale images and color components score fusion**

| | GPDS-CL1 | | Bogazici | |
|---|---|---|---|---|
| | **MSIFT** | **OLOF** | **MSIFT** | **OLOF** |
| **Gray** | 1.95 | 2.11 | 0.87 | 1.27 |
| **R+G+B** | 0.78↓60% | 1.61↓24% | 0.57↓34% | 0.94↓26% |
| **Y+Cb+Cr** | 1.22↓37% | 1.40↓34% | 0.28↓68% | 0.56↓60% |
| **H+S+V** | 0.96↓51% | 1.63↓23% | 0.26↓70% | 0.68↓46% |

Our experiments suggest that the feature extraction and acquisition condition (including sensor and environments conditions) highly influence the effectiveness of color representation for the palmprint identification. Our further research efforts are focused to develop color normalization approach which can be more independent to the sensor and nature of extracted features.

## 9. REFERENCES


[1] J. Chen and Y. S. Moon, "Using SIFT features in palmprint authentication," *Proc. 19th ICPR 2008*, Tempa (Florida), pp. 1-4, Dec. 2008.

[2] Z. Sun, T. Tan, Y. Wang, and S. Z. Li, "Ordinal palmprint representation for personal identification," *Proc. CVPR 2005*, vol. 1, pp. 279- 284, 2005.

[3] I. Fratric, and S. Ribaric, Colour-based palmprint verification – An experiment" *Proc. 14th IEEE Mediterranean Electrotechnical Conf.*, pp. 890–895. 2008.

[4] J. Zhou, D. Sun, Z. Qiu, K. Xiong, D. Liu, and Y. Zhang. "Palmprint Recognition by Fusion of Multi-color Components" *Proc. Intl .Conf. Cyber-Enabled Distributed Computing & Knowledge Discovery*, pp: 273 – 278, 2009.

[5] A. Morales, M. A. Ferrer and A. Kumar. "Improved Palmprint Authentication Using Contactless Imaging", *Proc. BTAS 2010*, Washington, Sep 2010.

[6] D. G. Lowe, 'Distinctive image features from scale-invariant keypoints', *Proc. IJCV 2004*, 2, (60), pp. 91-110. 2004.

[7] E. Konukoglu, E. Yorük, J. Darbon, B. Sankur, "Shape-Based Hand Recognition", *IEEE Trans. Image Processing*, 15(7), 1803-1815, 2006.

[8] G. S. Badrinath, P. Gupta, "Palmprint based Verification System Robust to Rotation, Scale and Occlusion" *Proc. 12th Intl. Conf. on Computer & Info. Tech. (ICCIT 2009),* pp. 408-413, 2009.